J. Membrane Biol. 173, 19–29 (2000)

The Journal of
Membrane
Biology

Cell Shrinkage is Essential in Lysophosphatidic Acid Signaling in Ehrlich Ascites Tumor Cells

S. Pedersen, E.K. Hoffmann, C. Hougaard, I.H. Lambert
August Krogh Institute, Department of Biochemistry, Universitetsparken 13, University of Copenhagen, DK-2100 Copenhagen Ø, Denmark

Received: 15 July 1999/Revised: 16 September 1999

Abstract. The present study aimed at elucidating the initial intracellular lysophosphatidic acid (LPA)-induced signaling events, in order to investigate the sequence in which LPA affects the intracellular concentration of free, cytosolic Ca^{2+}, $[Ca^{2+}]_i$, ion channels, the F-actin cytoskeleton, cell volume and the Na^+/H^+ exchanger. We found that stimulation of Ehrlich cells with LPA induced a transient, concentration-dependent increase in $[Ca^{2+}]_i$, which is due to Ca^{2+} release from intracellular Ins(1,4,5)P_3-sensitive stores as well as an influx of Ca^{2+}. The EC_{50} values for LPA-induced Ca^{2+} mobilization were estimated at 0.03 nM and 0.4 nM LPA in the presence and absence of extracellular Ca^{2+}, respectively. The LPA-induced increase in $[Ca^{2+}]_i$ resulted in (i) co-activation of Ca^{2+}-activated, charybdotoxin (ChTX)-sensitive K^+ and niflumic acid-sensitive Cl^- currents; (ii) a subsequent cell shrinkage and increased polymerization of F-actin, and (iii) activation of a Na^+/H^+ exchange, resulting in a concentration-dependent intracellular alkalinization. The EC_{50} value for the LPA-induced rate of alkalinization was estimated at 0.37 nM LPA. When cell shrinkage was prevented, the LPA-induced activation of the Na^+/H^+ exchanger was impaired. In conclusion, the initial signaling events induced by LPA involves activation of volume regulatory mechanisms.

Key words: Lysophosphatidic acid — $[Ca^{2+}]_i$ — Whole cell currents — pH_i — F-actin cytoskeleton

Introduction

Lysophosphatidic acid (LPA) is a lipid messenger with prominent cellular effects (*see* Moolenaar et al., 1997), which generally fall into two categories: (i) effects related to cell growth, e.g., stimulation of proliferation, suppression of apoptosis and alteration of differentiation and (ii) effects dependent on the remodeling of the cytoskeleton, e.g., induction of secretion, shape changes, adhesion and contraction (*see* Goetzl & An, 1998). LPA is predominantly generated by a stimulated liberation of precursor phospholipids e.g., phosphatidic acid, which subsequently undergo enzymatic conversion to LPA by extracellular phospholipase A_2 (PLA_2) (*see* Goetzl & An, 1998).

Extracellularly applied LPA mediates its effects via a subfamily of G-protein coupled receptors, of which those encoded by the endothelial differentiation genes (*edgs*) at present are the better characterized (*see* Moolenaar et al., 1997; Goetzl & An, 1998). The LPA receptor couples to at least three different types of G-proteins: (i) $G_{\alpha q/11}$, leading to phospholipase C (PLC) activation, inositol 1,4,5-trisphosphate (Ins(1,4,5)P_3)-generation and subsequent release of intracellular Ca^{2+}, activation of mitogen activated protein (MAP) kinases, and activation of protein kinase C (PKC); (ii) $G_{\alpha i}$, generating a decrease in intracellular [cAMP] and activation of the ras-raf-MAP kinase pathway and (iii) $G_{\alpha 12/13}$, resulting in stimulation of the rho GTPase pathway, activation of phospholipase D and phosphatidyl inositol (PI) 3-kinase (*see* Moolenaar et al., 1997; Goetzl & An, 1998).

It has only recently become clear that regulation of cell growth and proliferation is tightly coupled to regulation of cell volume and ionic currents (Wonderlin & Strobl, 1997; Lang et al., 1998). Certain mitogens have been shown to induce an increase in the intracellular concentration of free cytosolic Ca^{2+}, $[Ca^{2+}]_i$, resulting in activation of Ca^{2+}-sensitive K^+ channels leading to transient cell shrinkage due to a net loss of KCl (*see* Lang et al., 1998). In addition, the increased $[Ca^{2+}]_i$ induces a depolymerization of the F-actin cytoskeleton in certain cells (e.g., Moran et al., 1996), whereas in others, includ-

Correspondence to: S. Pedersen

ing Ehrlich cells, shrinkage will result in F-actin polymerization (Pedersen, Mills & Hoffmann, 1999). These cytoskeletal rearrangements could be responsible for the activation of the Na^+,K^+,2Cl^- cotransporter and the Na^+/H^+ exchanger seen upon cell shrinkage (*see* Lang et al., 1998). This sequence of events is similar to that activated by cell shrinkage due to increased osmolarity, which is considered a fundamental mechanism of cell volume regulation (Hoffmann & Pedersen, 1998), supporting the idea that cell volume regulatory mechanisms might also be crucial for regulation of cell growth and proliferation (*see* Lang et al., 1998).

LPA is a known mitogen and several LPA-induced effects have been described, however, only little is known about the initial signaling events activated by LPA. Thus, the purpose of the present study is to elucidate whether LPA could induce its mitogenic effects via stimulation of the classical signaling pathway activated by osmotic shrinkage, by studying LPA-induced effects on $[Ca^{2+}]_i$, K^+ and Cl^- conductances, F-actin content, cell volume, the Na^+,K^+,2Cl^- cotransporter and the Na^+/H^+ exchanger.

A part of this investigation has been presented in an abstract form (Pedersen, Hoffmann & Lambert, 1999*a*, *b*).

Materials and Methods

Cell Suspension and Incubation Media

Ehrlich ascites tumor cells were maintained by weekly intraperitoneal transplantation in female white NMRI mice (25–30 g). One week after inoculation, the cells were harvested as described by Hoffmann, Lambert and Simonsen (1986). The cells were washed twice and resuspended at a cytocrit of 4% in standard Ringer (in mM: 143 NaCl, 5 KCl, 1 $MgSO_4$, 1 Na_2HPO_4, 1 $CaCl_2$, 3.3 MOPS, 3.3 TES, 5 HEPES, pH adjusted to 7.4 with NaOH) and preincubated 15–30 min before initiating the experiment. In Ca^{2+}-free media, Ca^{2+} was omitted and 2 mM EGTA added. In low-Na^+ medium, 142 mM NaCl was replaced by 142 mM NMDGCl. In 'high $[K^+]_o$' medium, 48 mM NaCl was replaced by 48 mM KCl, yielding a total $[K^+]_o$ of 53 mM. The experiments were executed at 37°C. For electrophysiological experiments, the cells were suspended at a cytocrit of 0.2–0.5% in standard Ringer. The internal pipette solution was of the following composition (in mM): 100 aspartic acid, 40 tris · HCl, 100 tris[hydroxymethyl]aminomethane, 1.2 $MgCl_2$, 0.1 EGTA, 10 HEPES, 2 Na_2ATP and pH adjusted to 7.4 with CsOH. Upon entering into the whole-cell configuration, the cells were superfused with a KCl-free solution containing only 10 mM NaCl (NaCl was replaced by equimolar amounts of NMDGCl), in order to suppress inward K^+ and Na^+ currents.

Reagents and Stock Solutions

Unless noted otherwise, all chemicals were purchased at Sigma Chemical (St. Louis, MO) and stored at −20°C. Silicone oil AR 200/200 was obtained from Serva (Heidelberg, Germany) and silicone oil DC 200/20 was purchased from Bie & Berntsen (Rødovre, Denmark). ^{3}H-inulin and $^{86}Rb^+$ were obtained from Amersham (Buckinghamshire, UK) and Risø (Roskilde, Denmark), respectively. Bumetanide (a gift from Leo Pharmaceuticals, Ballerup, Denmark), was kept as a 5 mM stock solution in 96% ethanol. Rhodamine-conjugated phalloidin, SlowFade™, BCECF-AM and fura-2-AM were obtained from Molecular Probes (Leiden, Holland) and the latter two were prepared in dry DMSO as a 1.6 mM and 1 mM stock solution, respectively. Thapsigargin (1 mM) and charybdotoxin (5 μM) were purchased from Alomone Labs (Jerusalem, Israel) and prepared as stock solutions in 96% ethanol and standard Ringer containing 0.5% BSA, respectively. EIPA (10 mM) and nigericin (1 mg/ml) were dissolved in 96% ethanol. Niflumic acid was prepared as stock solution in dry DMSO at a concentration of 500 mM.

Estimation of $[Ca^{2+}]_i$ Using Fura-2

Loading of the cells with fura-2-AM and measurement of $[Ca^{2+}]_i$ was conducted as previously described (Jørgensen, Lambert & Hoffmann, 1996). The fura-2 loaded cells were diluted to a cytocrit of 0.5% in the cuvette, and the fluorescence was measured using a PTI RatioMaster spectrophotometer. The fluorescence emission, collected at 510 nm after excitation at 340 and 380 nm, respectively, and corrected for extracellular fluorescence, was calibrated *in vitro* as described by Jørgensen et al. (1996), and $[Ca^{2+}]_i$ was calculated as described by Grynkiewicz, Ponie and Tsien (1985).

Estimation of pH_i

Loading of Ehrlich cells with 2′,7′-bis-(2-carboxyethyl)-5,6-carboxyfluorescein, tetraacetoxymethyl ester (BCECF-AM) and measurement of intracellular pH (pH_i) were conducted essentially as described by Pedersen et al. (1996). The BCECF loaded cells were diluted to a cytocrit of 0.3% in the cuvette, and the fluorescence was detected using a PTI RatioMaster spectrophotometer. The fluorescence emission was measured at 525 nm after excitation at 445 nm and 495 nm, respectively. Linear *in situ* calibration of the BCECF fluorescence signal to pH_i was performed after each experiment using the nigericin method (*see* Thomas et al., 1979), and three to four values of pH_o were used to construct the calibration curve. Extracellular fluorescence was subtracted from the recorded signal prior to calculation of the 445 nm/495 nm ratio.

Cell Volume

Cell volume was measured by electronic cell sizing using a Coulter Multisizer II (Coulter, Luton Beds) after dilution of the cells to a cytocrit of 0.016% in the experimental medium. The tube orifice was 100 μm, and the mean cell volume was calculated as the median of the cell volume distribution curves after calibration with latex beads (diameter 14.1 μm).

$^{86}Rb^+$ Efflux Measurements

The cells were equilibrated with $^{86}Rb^+$ (2×10^4 Bq/ml) for 40 min in standard Ringer, then washed once in standard Ringer and finally resuspended at a cytocrit of 2% in standard Ringer containing 30 μM bumetanide. Bumetanide was added in order to avoid any contribution to the $^{86}Rb^+$ flux from activity of the Na^+,K^+,2Cl^-- and the K^+,Cl^--cotransporters. Cell-free efflux medium was isolated serially, in order to follow the $^{86}Rb^+$ efflux over time, by centrifugation (15.000×*g*, 20 sec) of 500 μl aliquots of the cell suspension through a silicone oil phase (300 μl 5:1 w/w AR200/200 and DC 200/200). Extracellular $^{86}Rb^+$ activity was estimated as cpm/mg dry wt, and in these experi-

ments $^{86}Rb^+$ was regarded as a tracer for K^+. Estimation of cellular dry weight and K^+ activity was performed as previously described (Hoffmann & Lambert, 1983; Lambert, Hoffmann & Jørgensen, 1989). Cellular specific K^+ activity (cpm $^{86}Rb^+$ μmol K^+) was corrected for $^{86}Rb^+$ and K^+ trapped in the extracellular phase using ^{3}H-inulin as a marker (Hoffmann & Lambert, 1983).

K^+ efflux (μmol K^+/g dry wt/min) was calculated from the initial rate of $^{86}Rb^+$ efflux (cpm/g dry wt/min) after agonist stimulation, divided by the cellular specific K^+ activity (cpm $^{86}Rb^+$/μmol K^+). The agonist induced K^+ efflux was estimated as the difference between the agonist induced efflux and that induced by addition of vehicle. The flux experiments were executed at 37°C.

^{3}H-inulin and $^{86}Rb^+$ activities were measured in a liquid scintillation spectrometer (Packard 2000CA Tri-Carb Liquid Scintillation Analyzer) in channels ranging from 2.0 to 18.6 keV and 19 to 1500 keV, respectively, using Ultima Gold™ (Packard) as scintillation fluid.

The initial agonist induced $^{86}Rb^+$ efflux rate was estimated from extracellular $^{86}Rb^+$ activity (cpm/dry wt) at time zero and about 10 and 20 sec after stimulation. The $^{86}Rb^+$ activity at the time of stimulation was estimated from the activity in the cell-free medium prior to stimulation by fitting the data to an exponential function as previously described (Hoffmann, Simonsen & Sjöholm, 1979).

Electrophysiological Recordings

The Ehrlich cells were diluted in standard medium and placed on a poly L-lysine coated coverslip, mounted on the stage of a Zeiss Axiovert 10 inverted microscope. The cells were allowed to settle and subsequently superfused with a K^+-free, low-Na^+ solution. The pipette resistance was 4–6 MΩ. The current was monitored using an Axopatch 200B patch clamp amplifier (Axon Instruments, CA) and sampled at 1 msec intervals. The holding potential was −20 mV. The following voltage protocol was used and applied every 15 sec: a 300 msec step to −70 mV, a 100 msec step to −90 mV followed by a linear ramp to +110 mV. The liquid junction potential between the pipette and bath solutions was calculated at 14 mV, using pClamp 7.0 software, and the data corrected accordingly. The patch-clamp experiments were performed at room temperature (23°C).

Estimation of the Rate Constant for the Initial Taurine Efflux

Ehrlich cells at a cytocrit of 7% were loaded for 60 min with ^{14}C-taurine (0.5 μCi/ml suspension), packed by centrifugation (770×*g*, 1 min) and resuspended in isotonic NaCl solution. Cellular ^{14}C-taurine activity (cpm/g cell dry wt) was estimated as described by Hoffmann et al. (1979), using ^{3}H-PEG as a marker for extracellularly trapped ^{14}C-taurine. The efflux experiment was initiated by dilution of 1 ml of the cell suspension in 13 ml isotonic NaCl solution. For estimation of ^{14}C-taurine activity in the extracellular medium, 6 samples were taken within the first minute, drugs added and another 6 samples taken within the following minute. The cells were separated from the extracellular medium by centrifugation through a silicone oil phase (1 part 200 DC20, 10 parts AR 200). Aliquots of the cell suspension were taken in duplicate at the end of the efflux experiments for estimation of the protein content using the Lowry technique. ^{14}C-activity in the medium was detected in a liquid scintillation spectrometer (Packard 2000CA Tri-Carb Liquid Scintillation Analyzer), using Ultima Gold™ (Packard) as scintillation fluid. The rate constants for the initial taurine efflux (ml cell water/g cell dry wt per min) were estimated as described by Lambert and Hoffmann (1994), i.e., as the product of the cell water content (ml cell water/g dry wt) and the slope of the plot $(a^t_m - a^0_m/a^0_c)$ *vs.* time, where a^t_m and a^0_m are the ^{14}C-taurine activity (cpm/ml medium) in the extracellular medium at time *t* and zero, respectively, and where a^0_c is the intracellular ^{14}C-taurine activity at time zero.

Fixation of Cells and Visualization of F-actin Using Confocal Microscopy

The cells were suspended at a cytocrit of 4% and stimulated with varying concentrations of LPA. Two minutes after stimulation, aliquots of 1 ml were transferred to paraformaldehyde solution (final conc. of paraformaldehyde 2%). The cells were fixed 10 min at room temperature, 30 min on ice and washed three times and then resuspended in TBS buffer (in mM: 150 NaCl, 10 mM Tris-HCl, 1 mM $MgCl_2$, 1 mM EGTA, pH 7.3) containing 0.1% azide (w/v). The cells were kept at 4°C until use.

The fixed cells were washed and resuspended in TBS buffer containing 0.05% Triton ×-100 and incubated with 1 U/ml rhodamine-phalloidin solution for 30 min at room temperature. Subsequently, the cells were washed twice in TBS buffer and resuspended at a volume of 1 ml. 20 μl cells were transferred to a clean coverslip, 20 μl SlowFade™ was added, and the cells were mounted on glass slides equipped with spacers.

The cells were viewed using a 40×/1.25 NA plan aprochromat objective mounted on a Leica DM IRB/E microscope coupled to a Leica TCS-NT confocal laser scanning unit (Leica Lasertechnik GmbH, Heidelberg, Germany). Excitation- and emission wavelengths were 568 nm and 590 nm, respectively, and optical slice thickness was 1 μm.

Abbreviations

AM: acetoxymethyl ester; BCECF: 2′,7′-bis-(2-carboxyethyl)-5,6-carboxyfluorescein; BSA: bovine serum albumin; ChTX: charybdotoxin; DMSO: dimethylsulfoxide; EGTA: ethylene-glycol-bis-β-amino-ethyl-(ether)N,N,N′,N′-tetraacetic acid; EIPA: 5-(N-ethyl-N-isopropyl)-amiloride; ERK: extracellular signal-regulated kinase; HEPES: N-2-hydroxyethylpiperazine-N′-2-ethane sulfonic acid; Ins(1,4,5)P_3: inositol 1,4,5-trisphosphate; LPA: L-α-lysophosphatidic acid, 1-oleyl; MAP: mitogen-activated protein; MEK: MAP kinase/ERK kinase; MLC: myosin light chain; MOPS: 3-(N-morpholino)propanesulfonic acid; NMDGCl: N-Methyl-D-Glucamine Chloride; PI: phosphatidyl inositol; PLC: phospholipase C; TBS: tris buffered saline; TES: N-tris-(hydroxymethyl)methyl-2-aminoethane sulfonic acid.

Statistical Evaluation

Unless otherwise indicated, the values are presented as the mean ± SEM or as a representative trace with the number of independent experiments indicated. Statistical significance was tested with a Students *t*-test, and the significance level used was $P < 0.05$, unless noted otherwise.

Results

LPA-induced Ca^{2+} Mobilization in Ehrlich Cells

Figure 1*A* demonstrates that addition of 10 nM LPA to Ehrlich cells suspended in Ca^{2+}-containing medium (1

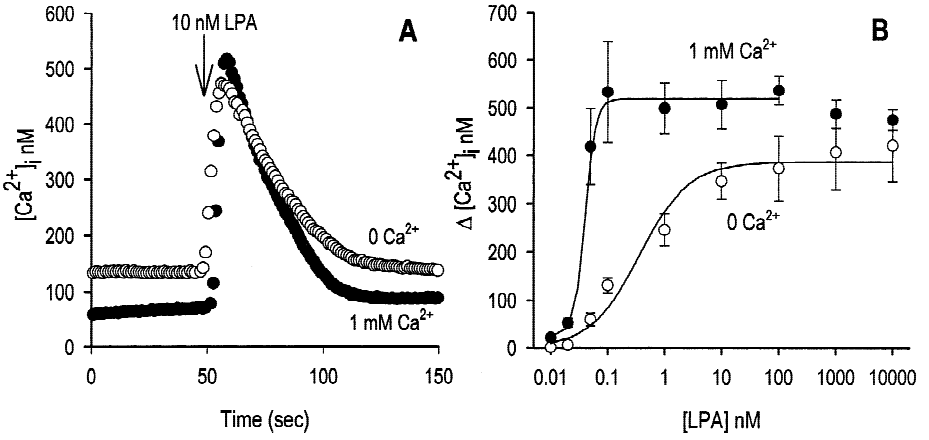

Fig. 1. The effect of LPA on $[Ca^{2+}]_i$ in the presence and absence of extracellular Ca^{2+}. $[Ca^{2+}]_i$ was measured in fura-2 loaded Ehrlich cells (*see* Materials and Methods). (Panel *A*) $[Ca^{2+}]_i$ was followed over time in Ehrlich cells suspended in Ca^{2+}-containing (1 mM, closed circles, $n = 3$) or Ca^{2+}-free (2 mM EGTA; open circles, $n = 4$) medium, and LPA was added as indicated by the arrow. (Panel *B*) Concentration-dependency of the LPA-induced increase in $[Ca^{2+}]_i$ estimated in the presence (closed circles) or in the absence (open circles) of extracellular Ca^{2+}. Each data point represents three to six independent experiments.

mM) induced a transient increase in the intracellular concentration of free, cytosolic Ca^{2+}, $[Ca^{2+}]_i$, which was reduced in the absence of external Ca^{2+} (2 mM EGTA), indicating that LPA induces a release of Ca^{2+} from internal stores as well as an influx of Ca^{2+}. The LPA-induced increase in $[Ca^{2+}]_i$ was found to be concentration-dependent both in the presence and absence of external Ca^{2+}, as seen in Fig. 1*B*. The data obtained in the absence of extracellular Ca^{2+} were fitted to the Michaelis-Menten equation: $\Delta[Ca^{2+}]_i = (\Delta[Ca^{2+}]_{i,max} \cdot [LPA]/(EC_{50} + [LPA])$, and the EC_{50} value was estimated at 0.4 nM LPA ($r = 0.986$). However, the data obtained in Ca^{2+}-containing medium was of a more complex nature, presumably due to cooperativity between the LPA-induced Ca^{2+} influx and release. Hence, the data obtained using 0–100 nM [LPA] were fitted to the Hill equation: $\Delta[Ca^{2+}]_i = (\Delta[Ca^{2+}]_{i,max} \cdot [LPA]^b)/(EC_{50}{}^b + [LPA]^b)$. The EC_{50} value was estimated at 0.03 nM LPA and b was estimated at 4, suggesting some cooperativity ($r = 0.997$). At [LPA] > 100 nM the values obtained in Ca^{2+}-containing medium decreased with increasing [LPA], and at 1 μM and 10 μM LPA, there was no significant difference between the LPA-induced increase in $[Ca^{2+}]_i$ in the presence and absence of external Ca^{2+}, respectively, suggesting that the LPA-activated Ca^{2+}-influx is reduced. This is confirmed in Fig. 2 in which Ehrlich cells suspended in Ca^{2+}-containing medium (1 mM) were exposed to 500 nM thapsigargin prior to stimulation with LPA. Thapsigargin is a well known inhibitor of the sarco-/endoplasmic Ca^{2+}-ATPase (SERCA) responsible for Ca^{2+} re-uptake into the intracellular Ins(1,4,5)P_3-sensitive stores. Thus, addition of thapsigargin ultimately leads to depletion of these stores (Thastrup et al., 1990), resulting in store depletion-activated Ca^{2+}-entry. This has been described in other

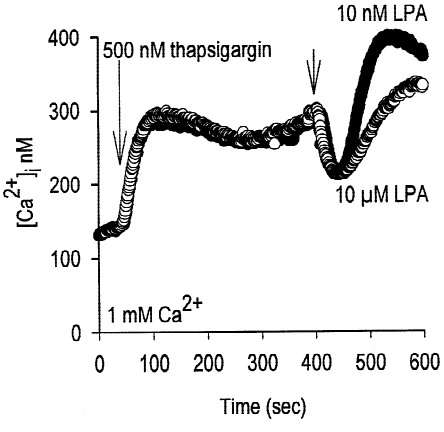

Fig. 2. LPA in low concentrations stimulates Ca^{2+} influx. The intracellular Ins(1,4,5)P_3-sensitive Ca^{2+} stores were depleted by addition of 500 nM thapsigargin, as indicated by the first arrow, leading to activation of the store depletion-activated Ca^{2+} influx in Ehrlich cells suspended in Ca^{2+}-containing medium (1 mM). After depletion of the stores, either 10 nM LPA (closed circles) or 10 μM LPA (open circles) was added, as indicated by the arrow. The traces shown represents six independent experiments.

cell types (Toescu & Petersen, 1994) as well as in Ehrlich cells (Pedersen et al., 1997; Pedersen et al., 1998*b*). When the thapsigargin-treated Ehrlich cells were stimulated with LPA as shown in Fig. 2, an initial decrease in $[Ca^{2+}]_i$ was seen, presumably due to a decreased influx of Ca^{2+} as a consequence of cell shrinkage (*see* Pedersen et al., 1998*a* for details). This LPA-induced decrease in $[Ca^{2+}]_i$ was followed by an increase $[Ca^{2+}]_i$ which seemed to be inversely concentration-dependent: lower [LPA] (<100 nM) seemed to be able to restore $[Ca^{2+}]_i$ and to induce an additional increase in

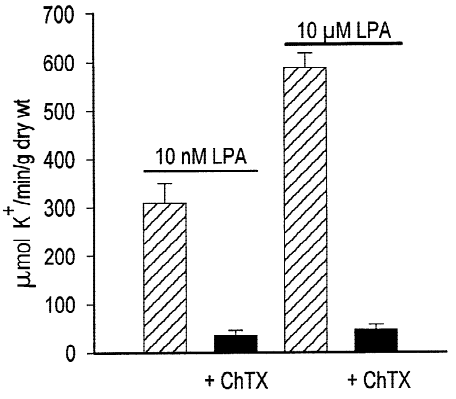

Fig. 3. The effect of charybdotoxin on the LPA-induced K^+ efflux. The LPA-induced K^+ efflux was measured using $^{86}Rb^+$ as a tracer for K^+, and the K^+ efflux was subsequently calculated as described in Materials and Methods. The LPA-induced K^+ efflux was estimated as the difference between the K^+ efflux induced by LPA and that induced by addition of the vehicle. The LPA-induced K^+ efflux activated by 10 µM LPA was significantly different from that induced by 10 nM LPA ($P = 0.0014$), and both were significantly reduced in the presence of 100 nM ChTX (10 µM LPA, $P < 0.0001$; 10 nM LPA, $P = 0.0006$). The data represent four independently executed experiments.

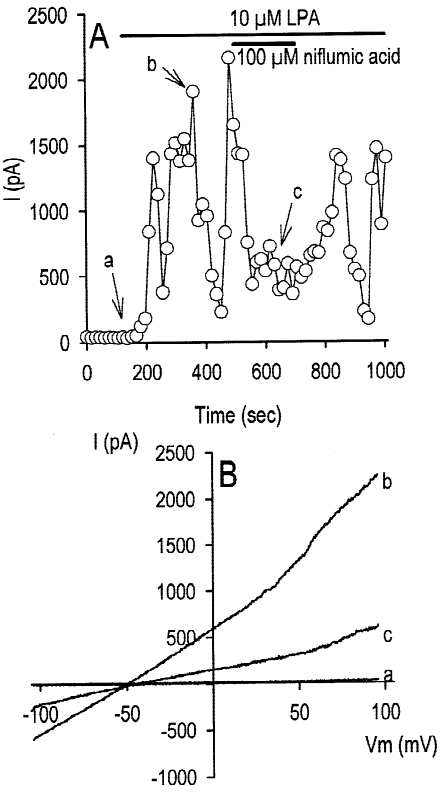

Fig. 4. Effects of LPA on the whole cell chloride current. (Panel *A*) The average whole cell current in a small window at +95 mV followed over time. The Ehrlich cells were superfused with K^+-free, low-Na^+ solution, and, subsequently, with the same solution containing either 10 µM LPA alone or 10 µM LPA and 100 µM niflumic acid, as indicated by the bars. (Panel *B*) The reconstructed *IV*-curves for the whole cell current recorded at the time points a, b and c, as indicated by the arrows in Panel *A*. E_{Cl} was estimated at −47 mV. The data represent four independent experiments.

$[Ca^{2+}]_i$, whereas upon addition of higher LPA concentrations (>100 nM) the $[Ca^{2+}]_i$ was restored but there was no additional increase in $[Ca^{2+}]_i$. This is in accordance with the finding that at [LPA] higher than 100 nM, the LPA-induced Ca^{2+} influx was reduced (*see* Fig. 1), but the underlying mechanism was not investigated further in the present study. Since LPA is known to activate the MAP kinase cascade, we investigated the effect of the various inhibitors of this cascade on the LPA-induced increase in $[Ca^{2+}]_i$. Neither PD98059, an inhibitor of MAP kinase activation (Dudley et al., 1995; 5 µM, 1½ hr, $n = 2$), nor SB 203580, which inhibits p38 MAP kinase (Cuenda et al., 1995; 10 µM, 1 hr, $n = 3$), had any detectable effect on the LPA-induced increase in $[Ca^{2+}]_i$, which could be taken to indicate that MAP kinase activation is downstream to Ca^{2+} mobilization.

Effects of LPA on K^+, Cl^- and Taurine Efflux

Generally, an increase in $[Ca^{2+}]_i$ induced by a mitogen will subsequently activate Ca^{2+}-dependent ion channels, primarily K^+ and Cl^- channels (*see* Lang et al., 1998). In agreement with this, Fig. 3 demonstrates that addition of LPA (10 nM and 10 µM) accelerated a bumetanide-insensitive K^+ efflux from Ehrlich cells in a concentration-dependent manner. This LPA-induced K^+ efflux could be inhibited by charybdotoxin (ChTX), which has previously been demonstrated to inhibit a Ca^{2+}-activated K^+ efflux pathway (Harbak & Simonsen, 1995; Hoffmann, 1999) as well as a Ca^{2+}-activated K^+ current ($I_{K,Ca}$, Riquelme et al., 1997) in Ehrlich cells. Furthermore, in two experiments 20 nM ChTX also inhibited the LPA (10 nM)-induced cell shrinkage (*data not shown*). The results shown in Fig. 3 are therefore taken to indicate that the LPA-induced K^+ efflux is predominantly due to activation of $I_{K,Ca}$.

To investigate the effects of LPA on the Cl^- conductance, whole cell patch clamp experiments were performed, in which K^+ and Na^+ currents were suppressed in order to allow us to follow only the development of the whole cell Cl^- current (I_{Cl}). Figure 4 demonstrates that addition of LPA activated an I_{Cl} of an oscillatory nature. In unstimulated cells, I_{Cl} was estimated at 84 ± 24 pA ($n = 4$), and upon stimulation with 10 µM LPA the maximal I_{Cl} was estimated at 3235 ± 453 pA ($n = 4$). The LPA-induced increase in I_{Cl} could be reversed and was inhibited reversibly by 78 ± 0.9% ($n = 4$) upon addition of 100 µM niflumic acid. In addition, 100 µM niflumic acid was able to inhibit the cell shrinkage induced by 10 nM LPA ($n = 2$, *data not shown*). Niflumic acid has previously been shown to inhibit a Ca^{2+}-activated I_{Cl}

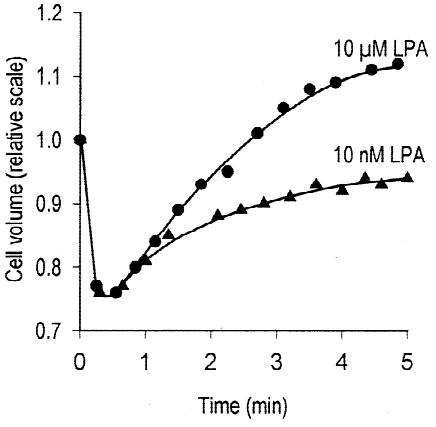

Fig. 5. Effect of LPA on cell volume. Cell volume was measured as a function of time by electronic cell sizing using a Coulter Multisizer II. The cells were diluted into the experimental buffer and LPA (10 nM or 10 μM) added at time zero. 10 nM LPA and 10 μM LPA induced a 19 ± 3% and 19 ± 4% cell shrinkage, respectively. The data are representative of three independent experiments.

($I_{Cl,Ca}$) by 60% in these cells (Pedersen et al., 1998*c*), indicating that LPA activates $I_{Cl,Ca}$ in Ehrlich cells.

Another important osmolyte in Ehrlich cells is the organic osmolyte taurine (Hoffmann & Lambert, 1983). In contrast to the inorganic osmolytes K^+ and Cl^- addition of 5 μM LPA had no significant effect on the unidirectional efflux of taurine, i.e., the rate constant was estimated at 0.12 ± 0.017 ml cell water/g cell dry wt/min ($n = 9$) under control conditions and at 0.14 ± 0.004 ml cell water/g cell dry wt/min ($n = 4$), in cells stimulated with 5 μM LPA.

Taken together, these findings indicate that the LPA-induced increase in $[Ca^{2+}]_i$ is a prerequisite for the subsequent activation of Ca^{2+}-dependent K^+ and Cl^- channels.

Effects of LPA on Cell Volume, the F-actin Cytoskeleton and pH_i

Activation of Ca^{2+}-dependent K^+ and Cl^- efflux pathways upon mitogenic stimuli will often lead to cell shrinkage. In Fig. 5 it is demonstrated that addition of LPA to Ehrlich cells also led to cell shrinkage, and that the LPA-induced cell shrinkage was concentration-independent in the range 10 nM to 10 μM LPA. The LPA-induced cell shrinkage was followed by a recovery of cell volume, a regulatory volume increase (RVI) response, the rate of which seemed to be concentration-dependent. The RVI response in Ehrlich cells is generally due to activation of a Na^+,K^+,$2Cl^-$ cotransport mechanism as well as Cl^-/HCO_3^- and Na^+/H^+ exchangers, resulting in a net uptake of NaCl (*see* Hoffmann & Pedersen, 1998). However, if the activity of the Cl^-/HCO_3^- exchanger is restricted, e.g., by removal of extracellular HCO_3^-, shrinkage-induced activation of the Na^+/H^+ exchanger will not contribute to the RVI response but instead result in intracellular alkalinization (*see* Hoffmann, 1997). In accordance with these findings, we found that when Ehrlich cells were suspended in low-Na^+ medium, thus preventing any Na^+,K^+,$2Cl^-$ cotransporter activity, LPA-induced cell shrinkage did not induce any RVI response (*data not shown*). This is taken to indicate that cell shrinkage induced by LPA could lead to activation of the same transport mechanisms as those responsible for restoration of cell volume upon exposure to osmotic shrinkage.

Many of the cellular effects induced by LPA are known to depend on remodeling of the cytoskeletal filaments (*see* Moolenaar et al., 1997; Goetzl et al., 1998), and a general feature of mitogens is that they affect F-actin polymerization (*see* Lang et al., 1998). By confocal visualization of F-actin in fixed Ehrlich cells incubated with rhodamine-conjugated phalloidin, as shown in Fig. 6*A*, we found that stimulation of Ehrlich cells with LPA induced no detectable qualitative changes in F-actin. However, by subsequent quantification of the F-actin content, as shown in Fig. 6*B*, we found that 10 μM LPA induced a quantitative increase in the F-actin content, suggesting that actin polymerization is increased.

In Fig. 7*A* it is seen that stimulation of Ehrlich cells with 10 μM LPA led to an initial acidification followed by an intracellular alkalinization, which was inhibited by 80 ± 1% in the presence of 10 μM EIPA. The alkalinization induced by 10 nM LPA was inhibited by 77 ± 3% in the presence of EIPA (10 μM). Since EIPA is a well known inhibitor of the NHE-1 or NHE-2 type Na^+/H^+-exchanger (Wakabayashi, Shigekawa & Possegur, 1997), it is suggested that LPA-induced cell shrinkage activates a Na^+/H^+-exchanger of the NHE-1 or NHE-2 type. The degree of Na^+/H^+-exchanger activity induced by LPA, expressed as the rate of intracellular alkalinization, was calculated as the slope of the linear fit of the measurements obtained 0–60 sec after the maximal acidification. The LPA-induced Na^+/H^+-exchanger activity was found to be concentration-dependent, as *seen* in Fig. 7*B*, and could be fitted to simple Michaelis-Menten kinetics: alkalinization rate = (max. alkalinization rate · [LPA])/(EC_{50} + [LPA]). The EC_{50} value, i.e., the [LPA] needed in order to induce an alkalinization rate half the size of the maximal alkalinization rate, was estimated at 0.37 nM LPA, and the maximal rate of alkalinization was estimated at 0.17 pH units/min ($r = 0.988$). It has been demonstrated that at an extracellular concentration of K^+, $[K^+]_o$, at exactly 53 mM, osmotic shrinkage of Ehrlich cells can be prevented (Hoffmann, 1993). Under these conditions, agonist-induced increases in $[Ca^{2+}]_i$ remains unaltered, but the agonist-induced cell shrinkage is completely abolished (Pedersen et al., 1998*a*, *b*). In Fig. 7*C*

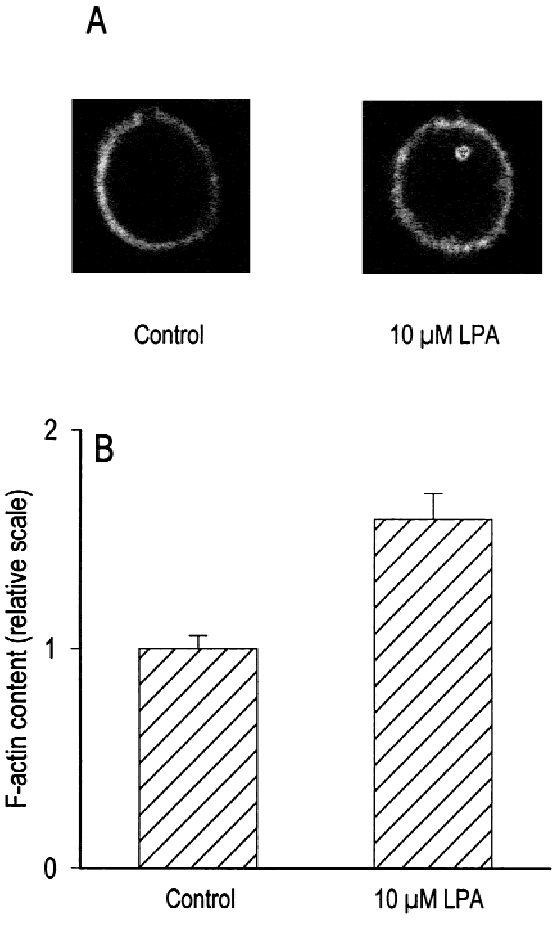

Fig. 6. Effect of LPA on the content of F-actin in Ehrlich cells. The cells were stimulated, fixed using 2% paraformaldehyde, and subsequently stained with rhodamine-conjugated phalloidin in order to label cellular F-actin. The F-actin was visualized using laser scanning confocal microscopy. (Panel *A*) Pseudo-color images showing the F-actin content of Ehrlich cells in the control situation and upon stimulation with LPA (10 nM and 10 μM). (Panel *B*) Quantification of the F-actin content in Ehrlich cells under control conditions and after stimulation with 10 μM LPA. The data presented represent 25 and 30 cells in the absence and presence of 10 μM LPA, respectively. The F-actin content in cells stimulated with 10 nM LPA was not significantly different from that in the control cells. However, in cells stimulated with 10 μM LPA, the F-actin content was significantly increased ($P = 0.0034$, Welch's *t*-test).

the Ehrlich cells are suspended in a 'high $[K^+]_o$' solution and it is seen that stimulation with 10 μM LPA does not lead to any activation of the Na^+/H^+ exchanger, thus, that LPA-induced activation of the Na^+/H^+ exchanger is secondary to cell shrinkage. Finally, we investigated the effect of inhibitors of the MAP kinase cascade on the LPA-induced alkalinization and found that neither PD98059 (5 μM, 1½ hr, $n = 2$), nor SB 203580 (10 μM, 1 hr, $n = 3$) had any detectable effect on the LPA-induced activation of the Na^+/H^+ exchanger, suggesting that shrinkage-induced activation of the Na^+/H^+ exchanger does not require MAP kinase activation.

Discussion

LPA Induces an Increase in $[Ca^{2+}]_i$ in Ehrlich Cells

It is well known that addition of LPA induces an increase in $[Ca^{2+}]_i$ in a wide variety of cell types (*see* Moolenaar et al., 1997; Goetzl et al., 1998). This also seems to be the case for the Ehrlich cells. Hence, in the present study, we find that addition of LPA to Ehrlich cells led to a concentration-dependent increase in $[Ca^{2+}]_i$ both in the presence and absence of extracellular Ca^{2+}, indicating that LPA activates Ca^{2+} influx as well as release of Ca^{2+} from internal stores (Fig. 1). The EC_{50} values for the LPA-induced increase in $[Ca^{2+}]_i$ was estimated at 0.03 nM and 0.4 nM in the presence and absence of external Ca^{2+}, respectively, indicating that LPA acts via a receptor with very high affinity for its substrate. These EC_{50} values are relatively close to that reported for LPA-induced Ca^{2+}-mobilization in human A431 carcinoma cells (0.2 nM, Jalink et al., 1995). However, in many other cell types, LPA was found to act via receptors with significantly lower affinity: e.g., in human foreskin fibroblasts the EC_{50} value was estimated at 20–30 nM LPA (Jalink, van Corven & Moolenaar, 1990), in rat mesangial cells at ~1 μM LPA (Inoue, Forster & Epstein, 1995), in kidney proximal tubular cells, at 2.6 μM LPA (Dixon, Young & Brunskill, 1999), and in human B lymphocytes, it was estimated at 42 nM LPA (Rosskopf et al., 1998).

LPA-induced K^+ Efflux $I_{Cl,Ca}$ Activation and Subsequent Cell Shrinkage

The aim of the present study is to clarify the initial signaling events induced by LPA in Ehrlich cells, in order to investigate whether they share any similarities to the mitogen-induced signaling cascade, which apparently is also crucial for cell volume regulation (Lang et al., 1998). The reason for this is that many of the later intracellular effects of LPA, e.g., induction of cell growth and proliferation (*see* Moolenaar et al., 1997; Goetzl & An, 1998), have recently been shown to be tightly coupled to regulation of cell volume and ionic currents (Wonderlin & Strobl, 1997; Lang et al., 1998). However, the early signaling events induced by LPA still remain less well characterized. In the present paper we demonstrate that stimulation of Ehrlich cells with LPA-induced transient cell shrinkage followed by a regulatory volume increase (RVI) response (Fig. 5), which is in accordance with previously reported effects of other growth factor-like Ca^{2+}-mobilizing agonists such as bradykinin, thrombin and LTD_4 (*see* Hoffmann, 1993; Hoffmann, Simonsen & Lambert, 1993; Jørgensen et al., 1997) on volume in Ehrlich cells. It should be noted that

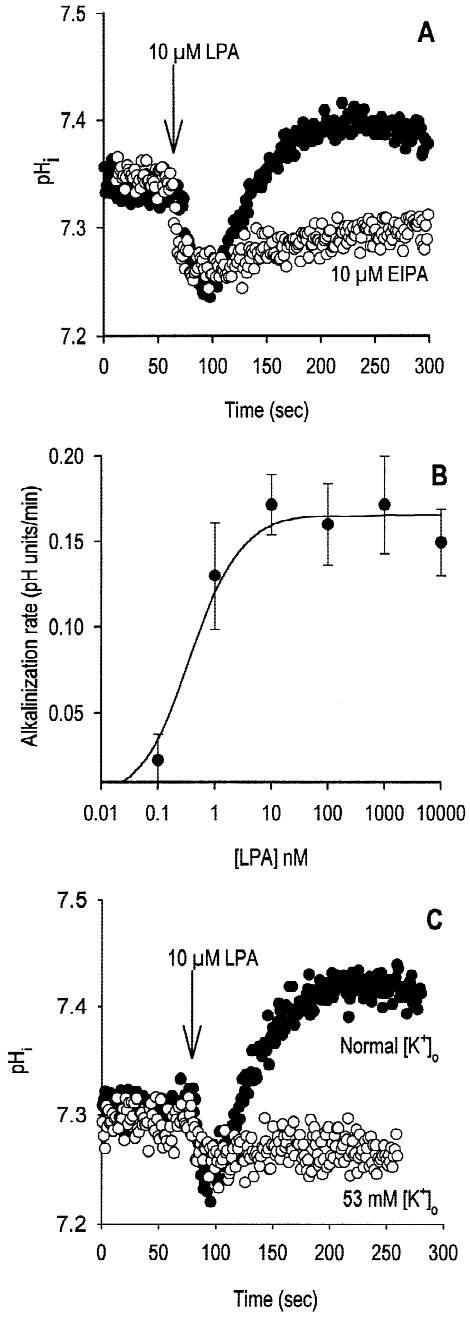

Fig. 7. LPA-induced cell shrinkage activates an EIPA-sensitive Na^+/H^+-exchanger. pH_i was measured in BCECF loaded Ehrlich cells, as described in Materials and Methods. (Panel *A*) pH_i was measured over time and 10 μM LPA was added as indicated by the arrow either in the absence (closed circles) or in the presence (open circles) of 10 μM EIPA. The data are representative of three independent experiments. (Panel *B*) Concentration-response curve for the LPA-induced activation of the Na^+/H^+-exchanger, measured as the slope of the linear fit obtained 0–60 sec after the maximal acidification. Each data point represents three to six independent experiments. (Panel *C*) pH_i was measured over time in Ehrlich cells suspended in standard Ringer (5 mM $[K^+]_o$, filled circles) or in 'high $[K^+]_o$' Ringer (53 mM $[K^+]_o$, open circles) to prevent cell shrinkage. The data represent three independent experiments.

the LPA-induced cell shrinkage is more pronounced than that elicited by bradykinin or thrombin. Agonist-induced shrinkage of Ehrlich cells has been demonstrated to be due to activation of Ca^{2+}-dependent K^+ and Cl^- efflux pathways (Hoffmann & Pedersen, 1999; Hoffmann, 1999). This also seems to be the case for LPA-induced cell shrinkage, because we were able to show that in addition to an increase in $[Ca^{2+}]_i$ (Fig. 1), LPA activated a Ca^{2+}-dependent K^+ efflux pathway sensitive to ChTX (Fig. 3) and an $I_{Cl,Ca}$, which could be inhibited by niflumic acid (Fig. 4). However, niflumic acid only blocked the LPA-induced activation of Ca^{2+}-dependent Cl^- currents by approx. 80%, which could be due to LPA-induced activation of niflumic acid-insensitive Ca^{2+}-activated Cl^- channels. A niflumic acid-sensitive $I_{Cl,Ca}$ whole cell current has previously been shown to become activated after even small increases in $[Ca^{2+}]_i$ in Ehrlich cells (Pedersen et al., 1998*c*). Interestingly, the LPA-activated $I_{Cl,Ca}$ seemed to oscillate, which might reflect that the LPA-induced increase in $[Ca^{2+}]_i$ in single cells also is of an oscillatory nature, but this remains to be investigated. This is taken to indicate that the LPA-induced activation of $I_{K,Ca}$ and $I_{Cl,Ca}$ is secondary to an increase in $[Ca^{2+}]_i$.

In several other cell types, LPA has been shown to activate either Cl^- or cation whole cell currents/conductive pathways. LPA activated a Ca^{2+}-activated Cl^- current, resulting in depolarization of the plasma membrane in *Xenopus* oocytes (Durieux et al., 1992), and in corneal keratocytes (Watsky, 1995), LPA was reported to activate a Cl^- current. In addition, LPA activated a Cl^- conductance in Rat-1 fibroblasts (Postma et al., 1996). However, LPA was recently reported to activate a K^+ current in NIH 3T3 mouse fibroblasts, leading to hyperpolarization of the plasma membrane (Repp et al., 1998) and to activate a K^+ current as well as a nonselective cation current in retinal pigment epithelium (Thoreson & Chacko, 1997). Thus, the present report is the first to demonstrate co-activation of Ca^{2+}-dependent K^+- and Cl^- currents by LPA.

Shrinkage-induced Stimulation of F-actin Polymerization and a Na^+/H^+ Exchanger

Certain mitogens are known to cause cytoskeletal rearrangements, and in accordance with this, many of the cellular effects of LPA have been shown to involve changes in cytoskeletal elements, e.g., shape changes, stress fiber formation, neurite retraction, and contraction (*see* Moolenaar et al., 1997; Goetzl & An, 1998). Several of the LPA-induced effects on the cytoskeleton are mediated via activation of rho, resulting in an increased phosphorylation of myosin light chain (MLC) and an increase in actomyosin contractility, leading to e.g., neurite retraction and stress fiber formation (*see* Moolenaar

et al., 1997). Our group has previously reported that the MLC kinase inhibitor ML-7 strongly inhibited shrinkage activation of the Na^+,K^+,$2Cl^-$ cotransporter (Krarup et al., 1998), but had no effect on the Na^+/H^+ activation induced by hypertonic cell shrinkage (Varming et al., 1998). In agreement with this, we find that ML-7 did not prevent LPA-induced cell shrinkage (2 μM, $n = 2$, *data not shown*). The majority of cell types in which the cytoskeleton-dependent effects of LPA have been investigated are adherent, which is in contrast to Ehrlich cells used in the present study. We found that stimulation of Ehrlich cells with LPA induced an increase in the content of F-actin (Fig. 4*B*), suggesting that LPA stimulates F-actin polymerization in these cells. In a recent report (Ren, Kiosses & Schwartz, 1999) it was demonstrated that LPA stimulates monomeric G-protein rho equipotently in adherent and suspended Swiss 3T3 cells, and that rho activity remains elevated in detached cells. Since rho activation induces polymerization of F-actin (*see* Mackay & Hall, 1998), LPA-induced F-actin polymerization in Ehrlich cells could be due to rho activation.

Hypertonic shrinkage of the Ehrlich cells also leads to an increase in F-actin content, which is most likely secondary to cell shrinkage (Pedersen at al., 1999). This supports the notion that addition of LPA stimulates the signaling cascade involved in regulation of cell volume, and that regulation of cell growth due to mitogenic stimulation might be tightly coupled to cell volume regulation.

In the present study we also found that the LPA-induced activation of the Na^+/H^+ exchanger was secondary to cell shrinkage, since it was abolished when cell shrinkage was prevented (Fig. 7*C*). Cell shrinkage has previously been shown to be a potent stimulus for activation of the Na^+/H^+ exchanger in Ehrlich cells (Pedersen et al., 1996; Pedersen et al., 1998*a, b*) and in other cell types as well (*see* Wakabayashi, Shigekawa & Pouysségur, 1997). In the present report we demonstrate that LPA had a biphasic effect on pH_i in Ehrlich cells: LPA induced an instant intracellular acidification followed by an alkalinization (Fig. 7*A*). Ca^{2+}-mobilizing agonists have previously been demonstrated to affect pH_i in a biphasic manner in these cells (Pedersen et al., 1998*a, b*), but the reason for the agonist-induced initial acidification remains somewhat obscure. Since the experiments in this study are performed in the absence of HCO_3^-, it seems unlikely that the LPA-induced acidification is due to activation of a Cl^-/HCO_3^- exchanger. Other mechanisms that might be involved in this acidification are discussed in (Pedersen et al., 1998*b*), of these the most likely seems to be an increased H^+ influx due to the agonist-induced hyperpolarization of the plasma membrane.

The LPA-induced alkalinization was inhibited by EIPA (Fig. 7*A*) and in 'high $[K^+]_o$' medium (Fig. 7*C*), suggesting that cell shrinkage activates a Na^+/H^+ exchanger of the NHE-1 and/or NHE-2 type (Wakabayashi et al., 1997). Both NHE-1 and NHE-2 have been identified in Ehrlich cells using polyclonal antiserum raised against these proteins (C. Varming, S.F. Pedersen and E.K. Hoffmann, *unpublished*). In Ehrlich cells, earlier findings have shown that an increase in $[Ca^{2+}]_i$ does not per se activate the Na^+/H^+ exchanger, but that the activation of the exchanger is secondary to Ca^{2+}-induced cell shrinkage (Pedersen et al., 1998*a, b*). Similar mechanisms of activation of the Na^+/H^+ exchanger have also been observed in other cell types after stimulation with mitogens and growth factors, e.g., by bradykinin in NIH 3T3 cells (Ritter et al., 1992; *see also* Wakabayashi et al., 1997), suggesting that it reflects a general and fundamental type of activation. It is unknown at present why the Na^+/H^+ exchanger remains activated even after cell volume has recovered. However, this could be related to the relatively slow reversibility of the shrinkage-induced increase in cortical F-actin content in Ehrlich cells (Pedersen et al., 1999).

To the knowledge of the authors, there are not yet many studies dealing with LPA-induced effects on pH_i. However, in hamster lung fibroblasts, addition of LPA led to intracellular alkalinization. This was found to be due to LPA-induced activation of a NHE-1 type Na^+/H^+ exchanger, which was shown necessary for rhoA-dependent LPA-induced stress fiber formation (Vexler, Symons & Barber, 1996).

LPA has been demonstrated to induce tyrosine phosphorylation of e.g., the epidermal growth factor receptor (Hackel et al., 1999). However, in Ehrlich cells it was previously demonstrated that tyrosine kinase inhibition had no effect on the Na^+/H^+ activation induced by hypertonic cell shrinkage (Varming et al., 1998). Thus, since hypertonic- and LPA-induced cell shrinkage seem to activate similar mechanisms, it seems unlikely that tyrosine kinase events induced by LPA should be upstream to activation of the Na^+/H^+ exchanger. Furthermore, LPA is known to activate the MAP kinase cascade, however we found no inhibitory effect of various blockers of the MAP kinase cascade on the LPA-induced effects on $[Ca^{2+}]_i$ and pH_i, which could suggest that LPA-induced MAP kinase activation is downstream to these events.

In conclusion, the present study aimed at elucidating the early LPA-induced signaling events in Ehrlich cells, and we found that (i) LPA was able to induce an increase in $[Ca^{2+}]_i$ due to release as well as influx of Ca^{2+}. The LPA-induced increase in $[Ca^{2+}]_i$ led to activation of a ChTX-sensitive K^+ efflux and a niflumic acid-sensitive Cl^- current, resulting in transient cell shrinkage. The LPA-induced cell shrinkage activated a Na^+/H^+ exchanger which, in turn, led to intracellular alkalinization.

The LPA-induced signaling in Ehrlich cells is very similar to that induced by hypertonic cell shrinkage, confirming the notion that regulation of these events are interrelated (*see* Lang et al., 1998).

The authors wish to thank Birgit B. Jørgensen for technical assistance. This work was supported by the Danish Natural Science Research Council (Grants 952762, 9601317, 9601404 and 9801946), The Carlsberg Foundation (Grants 960344/40-1099, 970438/40-1256) and the Novo Nordisk Foundation.

References

Cuenda, A., Rouse, J., Doza, Y.N., Meier, R., Cohen, P., Gallagher, T.F., Young, P.R., Lee, J.C. 1995. SB 203580 is a specific inhibitor of a MAP kinase homologue which is stimulated by cellular stresses and interleunin-1. *FEBS Lett.* **364:**229–233

Dixon, R.J., Young, K., Brunskill, N.J. 1999. Lysophosphatidic acid-induced calcim mobilization and proliferation in kidney proximal tubular cells. *Am. J. Physiol.* **276:**F191–F198

Dudley, D.T., Pang, L., Decker, S.J., Bridges, A.J., Saltiel, A.R. 1995. A synthetic inhibitor of the mitogen activated protein kinase cascade. *Proc. Natl. Acad. Sci.* **92:**7686–7689

Durieux, M.E., Salafranca, M.N., Lynch, K.R., Moorman, J.R. 1992. Lysophosphatidic acid induces a pertussis toxin-sensitive Ca^{2+}-activated Cl^- current in *Xenopus laevis* oocytes. *Am. J. Physiol.* **263:**C896–C900

Goetzl, E.J., An, S. 1998. Diversity of cellular receptors and functions for the lysophospholipid growth factors lysophosphatidic acid and sphingosine 1-phosphate. *FASEB J.* **12:**1589–1598

Grynkiewicz, G., Poenie, M., Tsien, R.Y. 1985. A new generation of Ca^{2+} indicators with greatly improved fluorescence properties. *J. Biol. Chem.* **260:**3440–3450

Hackel, P.O., Zwick, E., Prenzel, N., Ullrich, A. 1999. Epidermal growth factor receptors: critical mediators of multiple receptor pathways. *Curr. Opin. Cell Biol.* **11:**184–189

Harbak, H., Nielsen, D.K., Christensen, S., Simonsen, L.O. 1995. Cell volume-induced changes in phosphatidylinositol (4,5)bisphosphate in Ehrlich mouse ascites tumor cells. *J. Physiol.* **489P:**114P

Hoffmann, E.K. 1993. Control of volume regulatory ion transport processes in a mammalian cell: Signalling by secondary messengers. *Alfred Benzon Symposium* **34:**273–294

Hoffmann, E.K. 1997. Intracellular transmission in cell volume regulation in Ehrlich ascites tumor cells. *J. Exp. Zool.* **279:**398–414

Hoffmann, E.K. 1999. LTD_4 activates charybdotoxin-sensitive and -insensitive K^+ channels in Ehrlich ascites tumor cells. *Pfluegers Arch.* **438:**263–268

Hoffmann, E.K., Lambert, I.H. 1983. Amino acid transport and cell volume regulation in Ehrlich ascites tumor cells. *J. Physiol.* **338:**613–625

Hoffmann, E.K., Lambert, I.H., Simonsen, L.O. 1986. Separate, Ca^{2+}-activated K^+ and Cl^- transport pathways in Ehrlich ascites tumor cells. *J. Membrane Biol.* **91:**227–244

Hoffmann, E.K., Pedersen, S.F. 1998. Sensors and signal transduction in the activation of cell volume regulatory ion transport systems. *In: Cell Volume Regulation.* F. Lang, editor. pp. 50–78. Karger, Basel

Hoffmann, E.K., Simonsen, L.O., Lambert, I.H. 1993. *In:* Interactions Cell Volume-Cell function. F. Lang and D. Haussinger, editors. pp. 187–248. Springer Verlag, Berlin, Heidelberg

Hoffmann, E.K., Simonsen, L.O., Sjöholm, C. 1979. Membrane potential, chloride exchange, and chloride conductance in Ehrlich mouse ascites tumor cells. *J. Physiol. Lond.* **296:**61–84

Hoffmann, E.K., Sjöholm, C., Simonsen, L.O. 1983. Na^+, Cl^- cotransport in Ehrlich ascites tumor cells activated during volume regulation (regulatory volume increase). *J. Membrane Biol.* **76:**269–280

Inoue, C.N., Forster, H.G., Epstein, M. 1995. Effects of lysophosphatidic acid, a novel lipid mediator, on cytosolic Ca^{2+} and contractility in cultured rat mesangial cells. *Circ. Res.* **77:**888–896

Jalink, K., Hengeveld, T., Mulder, S., Postma, F., Simon, M., Chap, H., van der Marel, G., van Boom, J., van Blitterwijk, W., Moolenaar, W. 1995. Lysophosphatidic acid-induced Ca^{2+} mobilization in human A431 cells: structure-activity analysis. *Biochem. J.* **307:**609–616

Jalink, K., van Corven, E.J., Moolenaar, W.H. 1990. Lysophosphatidic acid, but not phosphatidic acid, is a potent Ca^{2+}-mobilizing stimulus for fibroblasts. Evidence for an extracellular site of action. *J. Biol. Chem.* **265:**12232–12239

Jørgensen, N.K., Christensen, S., Harbak, H., Brown, A.M., Lambert, I.H., Hoffmann, E.K., Simonsen, L.O. 1997. On the role of calcium in the regulatory volume decrease (RVD) response in Ehrlich mouse ascites tumor cells. *J. Membrane Biol.* **157:**281–299

Jørgensen, N.K., Lambert, I.H., Hoffmann, E.K. 1996. Role of LTD_4 in the regulatory volume decrease response in Ehrlich ascites tumor cells. *J. Membrane Biol.* **151:**159–173

Krarup, T., Jacobsen, L.D., Jensen, B.S., Hoffmann, E.K. 1998. $Na^+/K^+/2Cl^-$ cotransport in Ehrlich cells: regulation by protein phosphatases and kinases. *Am. J. Physiol.* **275:**C239–C250

Lambert, I.H., Hoffmann, E.K. 1994. Cell swelling activates separate taurine and chloride channels in Ehrlich mouse ascites tumor cells. *J. Membrane Biol.* **142:**289–298

Lambert, I.H., Hoffmann, E.K., Jørgensen, F. 1989. Membrane potential, anion and cation conductances in Ehrlich ascites tumor cells. *J. Membrane Biol.* **111:**113–131

Lang, F., Busch, G.L., Ritter, M., Völkl, H., Waldegger, S., Gulbins, E., Häussinger, D. 1998. Functional significance of cell volume regulatory mechanisms. *Physiol. Rev.* **78:**247–306

Mackay, D.J., Hall, A. 1998. Rho GTPases. *J. Biol. Chem.* **273:**20685–20688

Moolenaar, W.H., Kranenburg, O., Postma, F.R., Zondag, G.C. 1997. Lysophosphatidic acid: G-protein signalling and cellular responses. *Curr. Opin. Cell. Biol.* **9:**168–173

Moran, J., Sabanero, M., Meza, I., Pasantes-Morales, H. 1996. Changes of actin cytoskeleton during swelling and regulatory volume decrease in cultured astrocytes. *Am. J. Physiol.* **271:**C1901–1907

Pedersen, S., Hoffmann, E.K., Hougaard, C., Jørgensen, N.K., Wybrandt, G.B., Lambert, I.H. 1997. Leukotriene D_4-induced Ca^{2+} mobilization in Ehrlich ascites tumor cells. *J. Membrane Biol.* **155:**61–73

Pedersen, S., Hoffmann, E.K., Lambert, I.H. 1999*a*. Lysophosphatidic acid-induced effects on volume, pH_i and $[Ca^{2+}]_i$ in Ehrlich ascites tumor cells. *Physiol. Res.* **48:**S106

Pedersen, S., Hoffmann, E.K., Lambert, I.H. 1999*b*. Intracellular signaling by lipid second messengers in Ehrlich ascites tumor cells. *Acta Physiol. Scand* **165:**CP21

Pedersen, S.F., Jørgensen, N.K., Hoffmann, E.K. 1998*a*. Dynamics of $Ca^{2+}{}_i$ and pH_i in Ehrlich ascites tumor cells after Ca^{2+}-mobilizing agonists or exposure to hypertonic solution. *Pfluegers Arch.* **436:**199–210

Pedersen, S.F., Kramhøft, B., Jørgensen, N.K., Hoffmann, E.K. 1996. Shrinkage-induced activation of the Na^+/H^+ exchanger in Ehrlich ascites tumor cells: Mechanisms involved in the activation and a role for the exchanger in cell volume regulation. *J. Membrane Biol.* **149:**141–159

Pedersen, S.F., Mills, J.W., Hoffmann, E.K. 1999. Role of the F-actin cytoskeleton in the RVD and RVI processes in Ehrlich ascites tumor cells. *Exp. Cell. Res.* **252:**63–74

Pedersen, S.F., Pedersen, S., Lambert, I.H., Hoffmann, E.K. 1998*b*. P2 receptor-mediated signal transduction in Ehrlich ascites tumor cells. *Biochim. Biophys. Acta* **1374:**94–106

Pedersen, S.F., Prenen, J., Droogmans, G., Hoffmann, E.K., Nilius, B. 1998*c*. Separate swelling- and Ca^{2+}-activated anion currents in Ehrlich ascites tumor cells. *J. Membrane Biol.* **163:**97–110

Postma, F.R., Jalink, K., Hengeveld, T., Bot, A.G.M., Alblas, J., de Jonge, H.R., Moolenaar, W.H. 1996. Serum-induced membrane depolarization in quiescent fibroblasts: activation of a chloride conductance through the G protein-coupled LPA receptor. *EMBO J.* **15:**63–72

Ren, X.D., Kiosses, W.B., Schwartz, M.A. 1999. Regulation of the small GTP-binding protein Rho by cell adhesion and the cytoskeleton. *EMBO J.* **18:**578–585

Repp, H., Koschinski, A., Decker, K., Dreyer, F. 1998. Activation of a Ca^{2+}-dependent K^+ current in mouse fibroblasts by lysophosphatidic acid requires a pertussis toxin-sensitive G protein and Ras. *Naunyn Schmiedebergs Arch. Pharmacol.* **358:**509–517

Ritter, M., Wöll, E., Häussinger, D., Lang, F. 1992. Effects of bradykinin on cell volume and intracellular pH in NIH 3T3 fibroblasts expressing the ras oncogene. *FEBS Lett.* **307:**367–370

Riquelme, G., Sepúlveda, F.V., Jørgensen, F., Pedersen, S., Hoffmann, E.K. 1998. Swelling-activated potassium currents of Ehrlich ascites tumor cells. *Biochim. Biophys. Acta* **1371:**101–106

Rosskopf, D., Daelman, W., Busch, S., Schürks, M., Hartung, K., Kribben, A., Michel, M.C., Siffert, W. 1998. Growth factor-like action of lysophosphatidic acid on human B lymphoblasts. *Am. J. Physiol.* **274:**C1573–C1582

Thastrup, O., Cullen, P.J., Drøbæk, B.K., Hanley, M.R., Dawson, A.P. 1990. Thapsigargin, a tumor promoter, discharges intracellular Ca^{2+} stores by specific inhibition of the endoplasmic reticulum Ca^{2+}-ATPase. *Proc. Natl. Acad. Sci. USA* **87:**2466–2470

Thomas, J.A., Buchsbaum, R.N., Zimniak, A., Racker, E. 1979. Intracellular pH measurements in Ehrlich ascites tumor cells utilizing spectroscopic probes generated in situ. *Biochemistry* **18:**2210–2218

Thoreson, W.B., Chacko, D.M. 1997. Lysophosphatidic acid stimulates two ion currents in cultured human retinal pigment epithelial cells. *Exp. Eye Res.* **65:**7–14

Toescu, E.C., Petersen, O.H. 1994. The thapsigargin-evoked increase in $[Ca^{2+}]_i$ involves an $InsP_3$-dependent Ca^{2+} release process in pancreatic acinar cells. *Pfluegers Arch.* **427:**325–331

Varming, C., Pedersen, S.F., Hoffmann, E.K., 1998. Protein kinases, phosphatases and the regulation of the Na^+/H^+ exchanger in Ehrlich ascites tumor cells. *Acta Physiol. Scand.* **163:**A24

Vexler, Z.S., Symons, M., Barber, D.L. 1996. Activation of Na^+-H^+ exchange is necessary for RhoA-induced stress fiber formation. *J. Biol. Chem.* **271:**22281–22284

Wakabayashi, S., Shigekawa, M., Pouysségur, J. 1997. Molecular physiology of vertebrate Na^+/H^+ exchangers. *Physiol. Rev.* **77:**51–74

Watsky, M.A. 1995. Lysophosphatidic acid, serum, and hyposmolarity activate Cl^- currents in corneal keratocytes. *Am. J. Physiol.* **269:**C1385–13893

Wonderlin, W.F., Strobl, J.S. 1996. Potassium channels, proliferation and G1 progression. *J. Membrane Biol.* **154:**91–107